

agrees very well with the (3.1 Mev) obtained in our calculation.  $E_{\text{corr}}$  is also shown on Fig. 1. It has a zero near the minimum of the second moment. Since  $E_{\text{corr}}^2$  is never greater than three percent of  $M_2$  the neglect of  $E_{\text{corr}}^2$  in the calculation of the second moment was justified. This small value of  $E_{\text{corr}}$  ensures, further, that the maxima of our partial strength functions occur near the energies,  $\epsilon_p$ , of the single-particle levels in the shell model.

The approximation methods used in the above calculation of the second moment are crude and can certainly be improved. The perturbation calculation for the core functions should be fairly accurate since the square integral,  $N_1^2$ , of the first-order wave functions,  $\Psi_0^{(1)}$ , is small.  $N_1^2$  is

$$N_1^2 = \beta^2 \sum_s \sum_{s'} \frac{v_{ss'}^2}{(\mathcal{E}_s - \mathcal{E}_{s'})^2} \quad (51)$$

where  $s$  and  $s'$  refer to occupied and unoccupied states respectively.  $N_1^2$  is found to be  $0.013 \beta^2$  so that  $\Psi_0^{(1)}$  is at least an order of magnitude smaller than  $\Psi_0^{(0)}$ .

the reduced mass  $m/2$  instead of the total mass of the nucleon,  $m$ , should be used in this calculation. Because of this Eq. (12) in the appendix of reference 9 must be divided by a further factor of 2.

The approximation involved in placing the extra nucleon,  $A$ , at the center of the core could be justified if the contributions of the various core nucleons to the second moment were proportional to their densities at the center of the core. The argument for this justification would be similar to that which was used in the preceding sections to show that  $\epsilon_c(\mathbf{x}_A)$  was constant over most of the volume of the core. At the center of the core the relative densities of the  $1s$ ,  $2s$ , and  $3s$  nucleons are, respectively, 1, 4, and 9. As seen on Fig. 1, the contributions of these nucleons to the second moment have these relative values for  $\beta=0$ . For other values of  $\beta$  the  $3s$  nucleons contribute a greater portion of the second moment. The extent to which this effect impairs the validity of the approximation used in the above calculation has not been investigated.

#### ACKNOWLEDGMENTS

The author is very pleased to thank Professor E. P. Wigner for suggesting this problem and for his help during the course of this work. Many parts of this work have benefited from discussions with Dr. R. G. Thomas, Dr. A. M. Lane, and Mr. J. Lascoux. The author is grateful to Princeton University for the award of an International Business Machines Corporation fellowship (1954-1955).

## Angular Distributions of the D+D Neutrons\*

PAUL R. CHAGNON† AND GEORGE E. OWEN  
The Johns Hopkins University, Baltimore, Maryland  
(Received October 10, 1955)

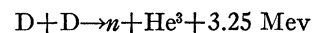
The angular distributions of the neutrons produced in the  $D(d,n)\text{He}^3$  reaction have been investigated experimentally in the deuteron energy range of 0.25 to 0.825 Mev. A two-crystal neutron spectrometer providing discrimination against gamma radiation was used as the detector. It is noted that the experimental data can be fitted by the deuteron stripping theory.

#### INTRODUCTION

ALTHOUGH the angular distributions of the neutrons from the reaction  $D+D \rightarrow \text{He}^3+n$  are of the greatest importance from both a theoretical and experimental standpoint, there is still some uncertainty in the experimental data. Konopinski *et al.*<sup>1</sup> have shown that the energy-dependence of the angular distribution coefficients can be accounted for by the differences in centrifugal barriers corresponding to the different components of the incident deuteron waves, provided that spin-orbit coupling is introduced. Conversely, the

experimentally observed energy dependence of the coefficients can be used to determine the amount of spin orbit coupling. In Konopinski's work no distinction is made between the  $D(d,n)\text{He}^3$  and  $D(d,p)\text{H}^3$  reactions. Fairbairn<sup>2</sup> has shown that the angular distributions of the neutrons from the reaction  $D(d,n)\text{He}^3$  can be fitted by deuteron stripping at energies above 4 Mev. The stripping calculation utilized an interaction radius of about  $4(10)^{-13}$  cm.

Recent experiments<sup>3-10</sup> on the reaction



\* This work was supported by the U. S. Atomic Energy Commission.

† National Science Foundation Fellow, 1953-1955. Present address: Physics Department, University of Michigan, Ann Arbor, Michigan.

<sup>1</sup> E. J. Konopinski and E. Teller, Phys. Rev. **73**, 822 (1948); Beiduk, Pruett, and Konopinski, Phys. Rev. **77**, 622 (1950); Pruett, Beiduk, and Konopinski, Phys. Rev. **77**, 628 (1950).

<sup>2</sup> Fairbairn, Proc. Phys. Soc. (London) **A67**, 990 (1954).

<sup>3</sup> G. T. Hunter and H. T. Richards, Phys. Rev. **76**, 1445 (1949).

<sup>4</sup> Blair, Freier, Lampi, Sleator, and Williams, Phys. Rev. **74**, 1599 (1948).

<sup>5</sup> J. Fuller and D. Ralph, Phys. Rev. **98**, 248(A) (1955).

<sup>6</sup> P. Baker, Jr., and A. Waltner, Phys. Rev. **83**, 1213 (1952).

<sup>7</sup> Manley, Coon, and Graves, Phys. Rev. **70**, 101(A) (1946).

fall roughly into two groups: those with incident deuteron energies below 100 keV and those where the incident deuteron energies were above 1 MeV. One set of experiments<sup>10</sup> was done between 150 keV and 465 keV.

In the experiments to be discussed, the deuteron energies ranged from 250 keV to 825 keV.

## EXPERIMENTAL ARRANGEMENT

### A. Target Chamber

Deuterons accelerated in the Van de Graaff generator of the Johns Hopkins physical laboratories were used to bombard deuterium gas contained in the target chamber shown in Fig. 1. A nickel foil nominally  $5 \times 10^{-5}$  in. thick retains the gas while permitting the accelerated deuterons to enter the target material. After passing through approximately 2 cm of gas, the deuterons stop in an aluminum disk. The stop is easily replaceable in case that an appreciable amount of deuterium becomes absorbed in it. The chamber was filled to a pressure of approximately 700 mm Hg with commercially prepared deuterium, 99.5% pure. The very thin foil holder and stop should have no appreciable effect on the neutrons produced in the reaction; the cylindrical symmetry of the outer brass chamber assures a negligible effect on the angular distribution up to angles of over  $165^\circ$ .

The same foil was used throughout the course of the experiments. An energy calibration for the machine was obtained by observing gamma-ray resonances from  $F^{19}(p,\alpha)O^{16}(\gamma)O^{16}$ . The foil was then inserted in the proton beam and the calibration repeated. The shift measured for those four resonances which were clearly observed was compared with a range-energy curve computed from the stopping power data quoted by Allison and Warshaw.<sup>11</sup> In this way the foil thickness was found to be  $1.62 \pm 0.05$  mg  $\text{cm}^{-2}$ . The energy loss for deuterons was then determined from these data. The energy loss in the target gas itself was also computed from the data given by Allison and Warshaw. This ranged from 100 to 225 keV for the various incident energies used in these experiments. The over-all error in the determination of the average deuteron energy in the target is estimated to be  $\pm 10$  keV.

### B. Current Measurement

The target chamber is insulated from ground to provide for measurements of the deuteron current reaching the target. A grounded aperture restricts the diameter of the beam so that all deuterons entering the target chamber must strike the foil.

A current integrator of the Elmore and Sands

<sup>8</sup> Eliot, Roaf, and Shaw, Proc. Roy. Soc. (London) A216, 57 (1953).

<sup>9</sup> I. Bartholdson, Arkiv Fysik 2, 271 (1950).

<sup>10</sup> Preston, Shaw, and Young, Proc. Roy. Soc. (London) 226, 212 (1954).

<sup>11</sup> S. K. Allison and S. D. Warshaw, Revs. Modern Phys. 25, 779 (1953).

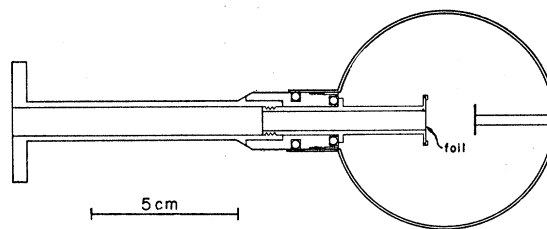


FIG. 1. The deuterium gas target chamber.

design<sup>12</sup> was used to measure the total charge carried to the target chamber by deuterons during the course of each run. The circuit also allows the mean potential of the target chamber to be so fixed as to minimize the effect of secondary electron emission and stray ion leakages.

The current integrator was calibrated by passing a steady current through it in series with a galvanometer whose accuracy is estimated to be  $\pm 2\%$ .

### C. Neutron Detector

Although only one neutron group results from  $D(d,n)He^3$ , there is some background consisting of neutrons and gamma rays from  $C^{12}(d,n)N^{13}$  and  $C^{12}(d,p)C^{13}$ , due to deposits of pump oil on the inner surfaces of the vacuum system. There is also capture radiation resulting from the capture of neutrons in the apparatus and in the walls of the room.

The neutron detector used was an improved model<sup>13</sup> of the two-crystal spectrometer<sup>14</sup> developed by the authors. It combines energy resolution with discrimination against gamma rays, thereby obviating the difficulties mentioned above. It is subject to a type of background due to chance coincidences, but this is easily distinguished from the real coincidence spectrum.

The efficiency of this detector has been calculated in detail<sup>13</sup>; it depends only on geometry and on the composition of the scintillators, except for one parameter related to the sensitivity of the coincidence circuit. This parameter could be measured indirectly; however, because of drifts in the electronics, it was found preferable to derive its value empirically from the angular distribution experiments themselves. In the D+D reactions, the initial state of the system is symmetrical, in the center-of-mass system, about a plane perpendicular to the beam axis; hence the angular distribution of the reaction products must also be symmetrical about this plane. For each series of runs, the value of the above-mentioned parameter was adjusted to make the result symmetrical about  $90^\circ$  in the center-of-mass system. The different values used corresponded to

<sup>12</sup> W. C. Elmore and M. Sands, *Electronics* (McGraw-Hill Book Company, Inc., New York, 1949).

<sup>13</sup> Chagnon, Owen, and Madansky, Rev. Sci. Instr. (to be published).

<sup>14</sup> Chagnon, Madansky, and Owen, Rev. Sci. Instr. 24, 656 (1953).

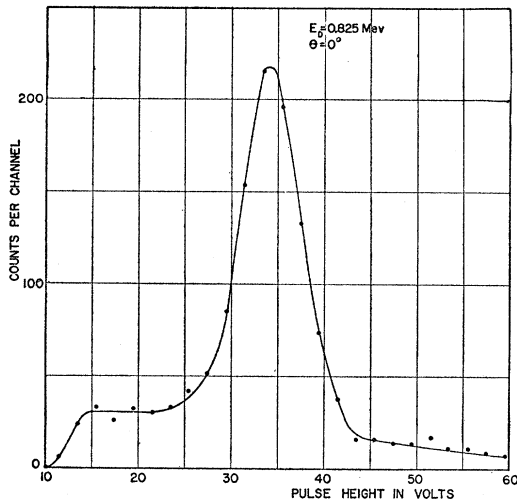


FIG. 2. A typical spectrum resulting from the neutrons from the D+D reaction as obtained with the fast coincidence spectrometer.

drifts in the average efficiency of not more than 9% from the mean value.

#### D. Experimental Details

For each of the bombarding energies, runs were made at nine angles. In most cases, each series of runs was repeated. The angles were measured to within  $\pm 1^\circ$ ; the angular definition was  $\pm 2^\circ$ . A fresh filling of deuterium was used each day, although leakage during the course of a day was less than  $\frac{1}{2}\%$  of the gas in the chamber.

A 100-channel pulse-height analyzer of the type originated by Wilkinson<sup>15</sup> and developed by Gatti<sup>16</sup> was used to analyze the pulses from the spectrometer. A typical spectrum shown in Fig. 2, illustrates the background subtraction. The shape of the background was obtained by operating the instrument at time delays different from the delay corresponding to the neutron time-of-flight. The known form of the background is fitted to the pulse-height spectrum in the regions on each side of the peak. The number of chance coincidence falling under the peak,  $A$ , is computed from this estimation; then the total number of counts in the region of the peak,  $T$ , is found by adding up the counts in the appropriate channels. The number of real coincidences,  $R$ , for this line is taken to be

$$R = T - A \pm (T + A)^{\frac{1}{2}}. \quad (1)$$

For each run, the statistical uncertainties are about  $\pm 3\%$ , but there is also some uncertainty due to the drift mentioned above. Therefore the errors were determined from the consistency of the data alone.

#### RESULTS

The data were analyzed from two points of view. First the data were fitted by the conventional least-

squares method, with an expression of the form

$$d\sigma/d\Omega = K(1 + A \cos^2\theta + B \cos^4\theta). \quad (2)$$

Experiments<sup>2,3</sup> carried out at higher energies have indicated no  $\cos^4\theta$  term below about 1.5 Mev. With the representation of Eq. (2), the "total cross section" is

$$\sigma_T = 4\pi K(1 + \frac{1}{3}A + \frac{1}{5}B). \quad (3)$$

The second type of analysis utilized was the deuteron stripping theory.<sup>17,18</sup> In the case of the reaction  $D(d,n)\text{He}^3$ , deuteron stripping can take place from either the incident deuteron or the target deuteron when viewed in the center-of-mass system. The differential cross section can be written

$$d\sigma/d\Omega = C\{G^2(K(\theta))j_0^2(k(\theta)R) + G^2(K(\pi-\theta))j_0^2(k(\pi-\theta)R)\}, \quad (4)$$

where  $G[K(\theta)] = 2(2\pi\alpha)^{\frac{1}{2}}/(\alpha^2 + K^2)$ ,  $j_0(k(\theta)R)$  is the spherical Bessel function of order zero,  $K(\theta) = \{k_n^2 + \frac{1}{4}k_d^2 - k_n k_d \cos\theta\}^{\frac{1}{2}}$ , and  $k(\theta) = \{k_d^2 + (4/9)k_n^2 - (4/3)k_n k_d \times \cos\theta\}^{\frac{1}{2}}$ .  $k_d$  and  $k_n$  are the wave numbers of the deuteron and neutron.

In this form, the theory assumes that the major portion of the interaction takes place between the "capturing nucleus" and the captured proton, while the interaction between the nucleus and outgoing neutron is small enough to be neglected.

This latter effect can be included as the "nuclear interaction term." Grant<sup>19</sup> has worked out the nuclear interaction term in a manner similar to that used by Bhatia<sup>18</sup> for the primary stripping. The major effect of this calculation in the case of the reaction  $D(d,n)\text{He}^3$  is to give a small isotropic component which can alter the spectrum a small amount mainly through interference.

The data were fitted consistently between 250 keV and 825 keV by neglecting the nuclear interaction term and using the differential cross section as given by Eq. (4). To obtain a reasonable fit with the data, it was necessary to allow  $R$ , the interaction radius, to increase slowly as one goes to lower energies.

The data and corresponding stripping fits are shown in Fig. 3. The ordinate  $W(\theta)$  is the differential cross

TABLE I. Coefficients  $K$ ,  $A$ , and  $B$  of Eq. (2) in the case of least-squares fitting, and  $R$  of Eq. (4) the case of fitting with the theory of deuteron stripping.

$E_d$ (Mev)	$(K \times 10^{27})$ $\text{cm}^2$	$A$	$B$	$(\sigma_T \times 10^{27})$ $\text{cm}^2$	$(R \times 10^{13})$ $\text{cm}$
0.250	1.44	$1.03 \pm 0.12$	$0.10 \pm 0.12$	25	8.2
0.400	2.23	$1.56 \pm 0.08$	$0.39 \pm 0.09$	45	8.0
0.500	2.64	$2.23 \pm 0.25$	$-0.07 \pm 0.28$	58	7.7
0.600	3.13	$2.08 \pm 0.10$	$0.36 \pm 0.10$	67	7.5
0.675	3.20	$1.46 \pm 0.22$	$1.22 \pm 0.23$	72	7.4
0.750	3.41	$1.87 \pm 0.29$	$1.21 \pm 0.30$	82	7.3
0.825	3.70	$0.60 \pm 0.16$	$2.06 \pm 0.18$	74	7.15

<sup>17</sup> S. T. Butler, Proc. Roy. Soc. (London) **A208**, 559 (1951).

<sup>18</sup> A. B. Bhatia *et al.*, Phil. Mag. **43**, 483 (1952).

<sup>19</sup> I. P. Grant, Proc. Phys. Soc. (London) **A67**, 981 (1954).

<sup>15</sup> D. Wilkinson, Proc. Cambridge Phil. Soc. **46**, 508 (1950).

<sup>16</sup> E. Gatti, Nuovo cimento **7**, 655 (1950).

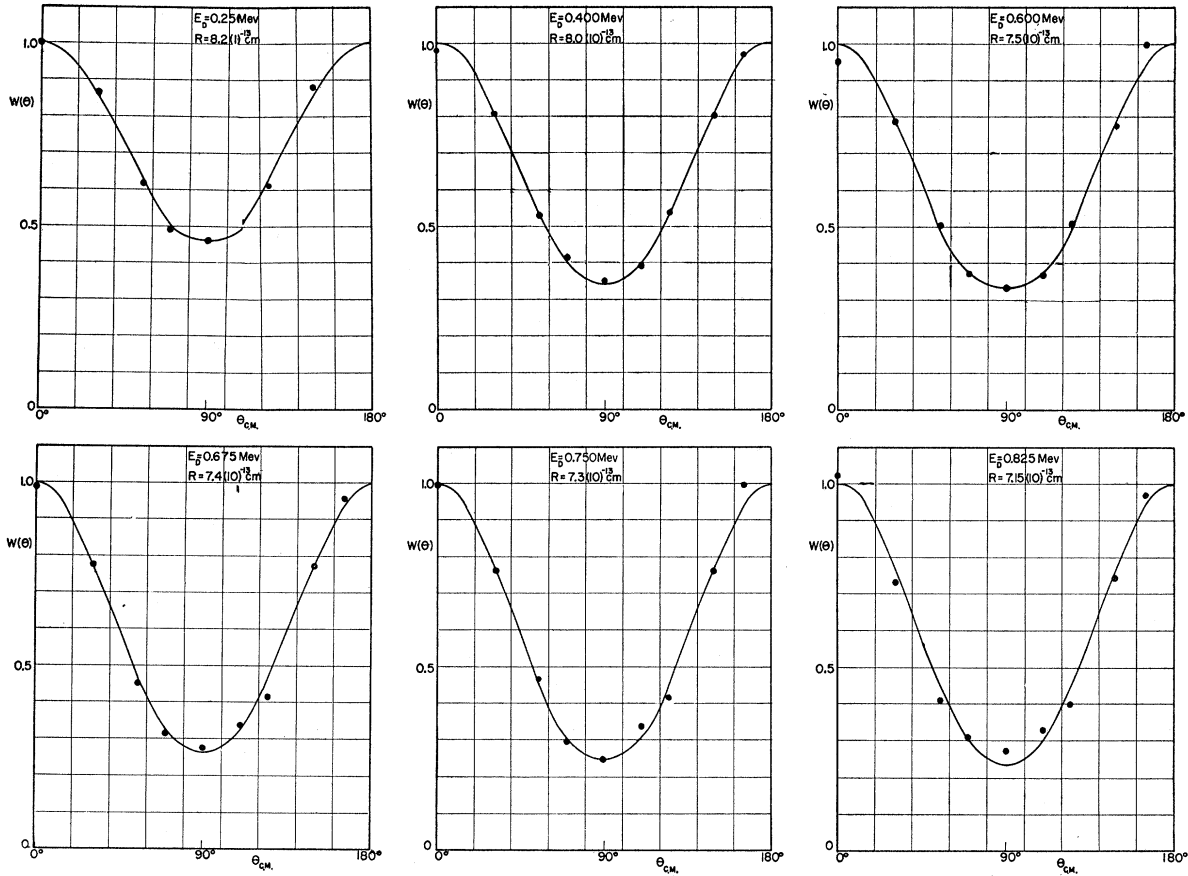


FIG. 3. The angular distributions of the D+D neutrons in the center-of-mass system as a function of the deuteron bombarding energy. The solid curves represent the deuteron stripping theory.

section normalized to 1 at  $\theta=0$ . The coefficients  $K$ ,  $A$ , and  $B$  in the case of the least-squares fitting, and  $R$  in the case of the fitting with the theory of deuteron stripping are given in Table I for each deuteron energy used. The total cross section is also listed and is shown in Fig. 4.

DISCUSSION

The results on  $\sigma_T$ ,  $K$ , and  $B$  are in good agreement with previous work; however, the values of  $A$  in the present measurements are noticeably larger than those of Hunter and Richards.<sup>2</sup> The background subtraction of the neutron spectrometer data is less subject to error than that of other detectors. An inherent background error will tend to produce angular distributions which have a larger amount of isotropy.

If indeed the deuteron stripping analysis is valid, the large value of  $R$  and the variation of  $R$  with energy may be accounted for if one assumes that deuteron stripping is not purely an interaction which takes place on the nuclear surface, but rather an interaction which also can take place when the two deuterons are at a distance which is large compared to the radius of the nuclear surface. In other words, the stripping can occur

both by interaction at the surface and by the "tunneling" of the proton across the space between the nuclear wells.

Let  $r$  be the radius of closest approach of the centers of mass of the two deuterons, and let the number of incident deuterons which come between  $r$  and  $r+dr$  be  $N(r)$ . If all deuterons between  $r=0$  and  $r=a$  interact by stripping at the surface with a probability  $\gamma$ , and if all deuterons which lie in the range  $r>a$  interact by tunneling with a probability  $\Gamma P(r)$ , then the average radius can be written as

$$\langle R \rangle = \frac{a \int_0^a N(r) dr + \frac{\Gamma}{\gamma} \int_a^\infty N(r) P(r) r dr}{\int_0^a N(r) dr + \frac{\Gamma}{\gamma} \int_a^\infty N(r) P(r) dr} \quad (5)$$

$N(r)$  will be a distribution which is similar to the classical Rutherford distribution and which gives the probability that a scattered particle will have a radius of closest approach between  $r$  and  $r+dr$ . The  $N(r)$  chosen will not cut off at  $zz'e^2/E_{e.m.}$ , but will have values down to  $r=0$ . The appendix provides a qualitative discussion

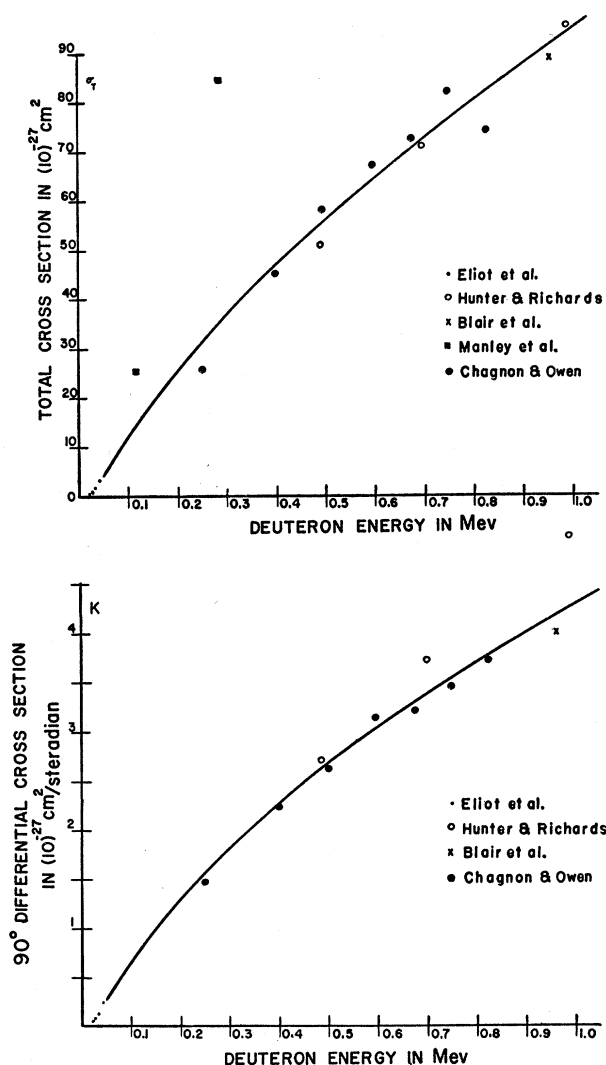


FIG. 4. The total cross section and 90° differential cross section for the reaction  $D(d,n)He^3$ .

of  $N(r)$  and indicates that the values of  $R$  and the variation of  $R$  with  $E_d$  can be fitted by an analysis of this type.

$P(r)$  is the tunneling probability, and to a first approximation goes as  $e^{-\alpha r}$ .

#### CONCLUSIONS

(1) The present results indicate less isotropy than previous work in the energy range from 250 keV to 825 keV.

(2) One of the most significant experimental facts which arises from the  $D+D$  reaction lies in the differences between the angular distributions for the  $(d,n)$  reaction and the  $(d,p)$  reaction. In spite of the fact that the total cross section for these two modes of reaction are very close at low energies, the  $(d,p)$  reaction shows a larger amount of isotropy.

If the nuclear reactions are charge-independent, the

difference must be explained solely by Coulomb effects. The suggestion of stripping might well account for these differences. If one modifies the wave function of the incoming deuteron such that the radius of interaction in the case of  $(d,p)$  stripping is slightly smaller than the radius of interaction for  $(d,n)$  stripping, the angular distribution of the protons certainly will be more isotropic than that for the neutrons at the same bombarding energy. This modification is not unreasonable, since one might expect, because of the Coulomb repulsion, the proton to be farther from the origin on the average.<sup>20</sup>

#### ACKNOWLEDGMENTS

Thanks are due Dr. L. Madansky, Dr. S. S. Hanna, Dr. R. Segel, and Dr. T. H. Berlin for many helpful discussions and comments, to Mr. J. Lambert for assistance in taking data, and to Mr. Paul Milich of the accelerator group.

#### APPENDIX

In the discussion of the parameters of Eq. (5), neutron stripping and proton capture from the incident deuteron will be considered.

If tunneling through the nuclear barrier is a process by which stripping can occur, a simple order of magnitude estimate indicates two things. First, the radius of interaction should be high at low energies where the tunneling process will predominate. Second, the average radius will decrease as the energy is increased. At energies of the order of ten times the Coulomb barrier height, the radius should become approximately constant and equal to the radius of the nuclear surface.

If the interaction time for the stripping is short compared to the time of transit of one deuteron past the other, the interaction can be treated as if the centers of mass of the two deuterons are stationary, with a center-of-mass separation  $r$ . The interaction time can be estimated by considering that the impulse  $\Delta p$  given to the outgoing neutron can arise only through the coupling  $\langle F \rangle$  between the proton and neutron in the deuteron. The average coupling force in a square well can be obtained by the impulse approximation. If  $\Delta p \sim (2MQ)^{\frac{1}{2}}$ , where  $Q$  is the  $Q$  value of the reaction, then

$$t = \Delta p / \langle F \rangle = 3.4 \times 10^{-24} Q^{\frac{1}{2}} \text{ sec}$$

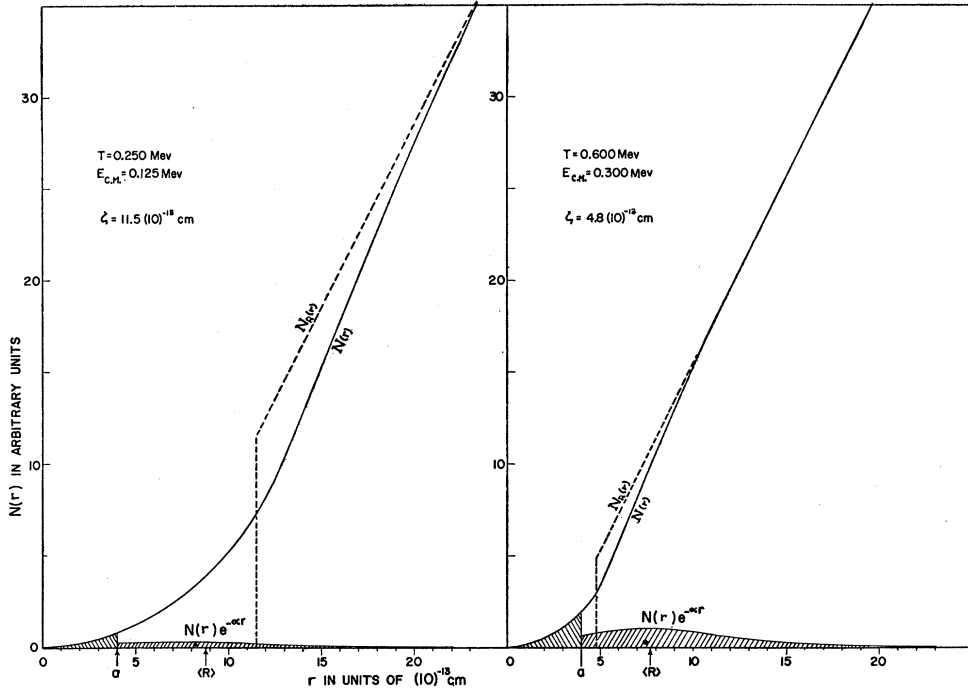
( $Q$  in MeV). The transit times are of the order  $10^{-21}$  sec; thus the adiabatic condition is satisfied.

The proton from one deuteron will tunnel to the  $He^3$  well, which the second deuteron presents, with a probability  $\Gamma P(r)$  which we shall assume is approximately like  $\Gamma e^{-\alpha r}$ , where  $r$  equals the center of mass separation of the two deuterons.<sup>21</sup>  $\Gamma P(r)$  is used when  $2r > a$ , where  $a$  is the radius of the nuclear surface.  $\alpha$  is

<sup>20</sup> J. R. Oppenheimer and M. Phillips, Phys. Rev. 48, 500 (1935).

<sup>21</sup> The exponential probability arises from a one-dimensional analysis.

FIG. 5. The distribution function  $N(r)$  for bombarding energies of 0.250 Mev and 0.600 Mev. The classical Rutherford distribution is shown. The shaded regions indicate the magnitude of the interaction as a function of  $r$ . If  $P(r) = \exp(-\alpha r)$ , where  $\alpha = 0.31 \times (10)^{13} \text{ cm}^{-1}$ , the calculated average  $R$  of the interaction is shown for  $\gamma = \Gamma = 1$ . These values are close to those obtained from the experimental data, which are indicated as dots in the shaded areas.



of the same order as  $2(2M\epsilon_d)^{1/2}\hbar$  given by  $\epsilon_d$ , the binding energy of the deuteron.

To consider the distribution function  $N(r)$  of the deuterons, let  $r$  equal the distance between the centers of mass at the point of closest approach. Then  $N(r)dr$  is the probability of finding the two deuterons with a separation between  $r$  and  $r+dr$ . Ultimately,  $N(r)$  should be obtained from the Schrödinger equation for the system. This distribution function must be evaluated at small  $r$  and also must contain a large number of angular momentum components. The essential points can be made without involving the details of the wave function.

A reasonable form of  $N(r)$  can be obtained from the following three constraints. First, the distribution function should be zero at  $r=0$ .

Second, let the distribution function go as the classical distribution for Rutherford scattering at large  $r$ :

$$N_R(r) = 2r - \zeta, \quad r \geq \zeta,$$

where  $\zeta = z z' e^2 / E_{c.m.}$ , and  $E_{c.m.}$  = the deuteron energy in the center-of-mass system. In this form,  $N_R(r)$  is the distribution in terms of the radii of closest approach of the classical orbits.

Third, the number of particles will be conserved. The classical distribution  $N_R(r)$  can be smeared out according to the wavelength  $\lambda$  of the deuteron. By folding  $N_R(r)$  with a Gaussian of width  $\lambda$ , one finds that the smeared distribution is essentially  $N_R(r)$  for values of  $r$  greater than  $2\lambda$ . The Gaussian, however,

does not conserve particles, therefore it is reasonable merely to find that curve which is zero at  $r=0$ , which approaches  $N_R(r)$  for  $r > 2\lambda$ , and which maintains the area under the distribution function constant.

If we now postulate that all deuterons which fall within  $r$  less than  $a$  (where  $a$  is the radius of the nuclear surface) will undergo stripping with a probability  $\gamma$ . All deuterons corresponding to  $r > a$  can interact by means of the tunneling mechanism,  $\Gamma P(r)$ , and the average radius of interaction is given by Eq. (5).

Figure 5 shows the constructed  $N(r)$  as a function of  $r$  for a bombarding energy of 600 kev and also for an incident deuteron energy of 250 kev. The shaded portions illustrate the magnitude of the interacting regions when  $\alpha = 0.31 \times 10^{13} \text{ cm}^{-1}$ ,  $\gamma = \Gamma = 1$ , and  $a = 4 \times 10^{-13} \text{ cm}$ .

Reasonable assumptions for  $a$ ,  $\alpha$ , and  $N(r)$  can provide a good fit to the values of  $R$  obtained from the experimental results. The qualitative nature of this calculation, however, is its major value. It does indicate that  $\langle R \rangle$  can be greater than  $a$  for low energies, and that  $\langle R \rangle$  under these conditions decreases to an asymptotic value approximately equal to  $a$  for higher energies. It should be noted that the denominator of Eq. (5) is the total number of interactions and therefore proportional to the total cross section.

The calculation is fairly sensitive to all of the parameters; thus the method does not warrant use in a quantitative analysis.